

# Phenomenological gravitational waveforms from spinning coalescing binaries

R. Sturani<sup>(1,2)</sup>, S. Fischetti<sup>(3)</sup>, L. Cadonati<sup>(3)</sup>, G. M. Guidi<sup>(1,2)</sup>, J. Healy<sup>(4)</sup>, D. Shoemaker<sup>(4)</sup>, A. Viceré<sup>(1,2)</sup>

(1) *Dipartimento di Scienze di Base e Fondamenti,*

*Università degli Studi di Urbino 'Carlo Bo', I-61029 Urbino, Italy*

(2) *INFN Sezione di Firenze, I-50019 Sesto Fiorentino, Italy*

(3) *Physics Department, University of Massachusetts, Amherst MA 01003, USA*

(4) *Center for Relativistic Astrophysics, Georgia Tech, Atlanta, GA 30332, USA\**

An accurate knowledge of the coalescing binary gravitational waveform is crucial for experimental searches as the ones performed by the LIGO-Virgo collaboration. Following an earlier paper by the same authors we refine the construction of analytical phenomenological waveforms describing the signal sourced by generically spinning binary systems. The gap between the initial inspiral part of the waveform, described by spin-Taylor approximants, and its final ring-down part, described by damped exponentials, is bridged by a phenomenological phase calibrated by comparison with the dominant spherical harmonic mode of a set of waveforms including both numerical and phenomenological waveforms of different type. All waveforms considered describe equal mass systems. The Advanced LIGO noise-weighted overlap integral between the numerical and phenomenological waveforms presented here ranges between 0.95 and 0.99 for a wide span of mass values.

PACS numbers: 04.30.Db,04.25.dg,,04.80.Nn

Keywords: gravitational waves, coalescing binaries, numerical waveforms, gravitational wave detection

## I. INTRODUCTION

The experimental program for gravitational wave detection is on the way, as the network of kilometer-scale interferometers formed by the Laser Interferometer Gravitational-wave Observatory (LIGO), Virgo and GEO are presently in science run or undergoing substantial upgrades taking them to their advanced version [1–3].

Among the possible sources one of the most promising is represented by the coalescence of compact binary systems of neutron stars or black holes. The coalescence of binary systems is usually described in terms of three distinct phases: the *inspiral*, the *merger* and the *ring-down*. The inspiral phase allows for an accurate analytical description via the so-called Post-Newtonian (PN) expansion, see for instance [4] for a review. The ring-down also admits a perturbative analytical model, as it describes the damped oscillations of the single object resulting from the binary coalescence, as a superposition of black-hole quasi-normal modes [5]. The merger phase is however fully non-perturbative and for generic systems it has not been described analytically but rather by numerical simulations.

During the last six years numerical relativity has made tremendous progress in describing the full coalescence of a binary system beginning with [6–8] and more recently [9–15], see [16–18] for reviews, and it can now produce waveforms for generic spin orientations, with moderate spin magnitude ( $\lesssim 0.9$ ) and mass ratios ( $\lesssim 10 : 1$ ).

Match-filtering techniques represent a powerful tool for seeking signals, but they need a detailed knowledge of the waveform in order to have high efficiency and to be useful for parameter estimation. They are extensively used in LIGO-Virgo experimental searches in order to uncover weak signals buried into noise, see e.g. [19] for the results of a recent match-filtered search. In such searches real data are compared with banks of template waveforms, made of a large number (tens of thousands) of templates: due to the computational cost of numerical simulations, it would be impractical to numerically generate the waveforms necessary to populate template banks.

There exist nowadays analytically constructed waveforms describing the entire coalescence of a binary system. They have been achieved in the Effective One Body (EOB) construction [20–23] for non-spinning systems, and in the EOB-spin waveforms [24], for binaries with spins aligned with the orbital angular momentum (thus non-precessing spins). In both cases of spinning and non spinning waveforms, a comparison with numerically generated waveforms is needed by the EOB construction in order to calibrate some free parameters of the model. Another method for generating analytical waveforms for spinning non-precessing binaries is by joining PN-generated inspiral with a fit of numerical waveforms to construct *phenomenological* waveforms, as done in [13]. In this paper, we further investigate on the family of phenomenological waveforms introduced in [25], dubbed PhenSpin, which are analytical waveforms describing the entire coalescence of *generically spinning* compact binaries. In particular a restricted set of

---

\*Electronic address: riccardo.sturani@uniurb.it

*phenomenological* waveforms [13] describing non-precessing systems are used here together with the same set of fully precessing numerical waveforms used in [25] to tune this new version of PhenSpin waveforms.

The PhenSpin waveforms have been constructed by joining the perturbative PN description of the inspiral to the ring-down phase by a phenomenological phase which plausibly describes the evolution of the waveform in between. With respect to the previous work introducing these waveforms, here we give a slightly modified (improved) version, identical in spirit but better tuned in some technical aspects, and produce new results assessing their faithfulness to numerical simulation in presence of detector noise. The improved details allow to obtain a slightly better match between the PhenSpin waveforms and the set of test waveforms they have been compared with.

Waveforms describing generically spinning coalescing binaries are not suitable for searches employing match-filtering, as the size of a template bank increases exponentially with the number of template parameters: since spinning waveforms depend on several parameters (masses, spin components of the binary constituents, angles defining the orientation of the source with respect to the observer) it is not practical to construct one template bank to cover the entire spin parameter space. Non spinning, or at least non-precessing waveforms, are usually preferred for template bank construction, with the exception of the so-called Physical Template Family, representing a single spin family waveform [26], which however can effectively describe also doubly spinning physical systems [27].

The availability of generically spinning waveforms is however badly needed to assess the efficiency of experimental searches based on banks of non-spinning templates, like [19]. Moreover fully spinning waveforms can be used as templates in connection with parameter estimation via Bayesian inference methods, which can be used as follow-up analysis to perform searches in the parameter space with full dimensionality, but restricted to a small subset of the entire space, as determined by lower level triggers.

The paper is organized similarly to [25] and the exposition has been kept here as self-contained as possible. In sec. II the analytical waveform construction and the waveforms used for calibration are revisited. Differences with respect to the old version of PhenSpin are described. In sec. III the results are presented, in the form of comparison between analytically and numerically generated waveforms, which reproduce the dominant quadrupolar mode  $l = m = 2$ . In sec. IV the conclusions that can be drawn from the present work are reported.

## II. THE METHOD

Following the original introduction of PhenSpin waveforms given in [25], the present work revisits the construction of analytical gravitational waveforms generated by the coalescence of spinning binary systems. The waveforms used to construct and calibrate our analytical model include the numerical waveforms used in the previous paper, describing equal mass binary systems ( $m \equiv m_1 = m_2$ ), with spin magnitudes  $|\mathbf{S}_1| = |\mathbf{S}_2| = 0.6 m^2$  and starting with  $\mathbf{S}_2$  orthogonal to the initial orbital angular momentum (where  $\mathbf{S}_{1,2}$  denote the binary constituent spin vectors and we posit  $G_N = c = 1$ ). Here in addition, to cover a portion of the parameter space not addressed by the numerical simulations, we use also four phenomenological waveforms of the type described in [13], generated via the LAL libraries [29] to calibrate the PhenSpin in the case of aligned spins, which together with the numerical relativity waveforms form our set of *test waveforms*.

The description of the dynamics adopted here models the inspiral phase via the standard TaylorT4 PN formulae, see [30] for definition and comparison of different PN approximants in the spin-less case. Un-like the non-precessing case, the knowledge of the time-varying amplitude and phase is necessary but not sufficient to determine the waveform from spinning precessing binaries, as it must be complemented by the spin and angular momentum evolution, see e.g. [31]:

$$\begin{aligned}\dot{\mathbf{S}}_{1,2} &= \boldsymbol{\Omega}_{1,2} \times \mathbf{S}_{1,2}, \\ \dot{\hat{\mathbf{L}}} &= -\frac{\nu}{v} (\dot{\mathbf{S}}_1 + \dot{\mathbf{S}}_2),\end{aligned}\tag{1}$$

where

$$\boldsymbol{\Omega}_{1,2} \equiv \left( \frac{3}{4} + \frac{\nu}{2} \mp \frac{3}{4}\delta \right) \hat{\mathbf{L}}_N\tag{2}$$

and  $\nu \equiv m_1 m_2 / M^2$  is the symmetric mass ratio and  $\delta \equiv (m_1 - m_2) / M$ , being  $M \equiv m_1 + m_2$  the total mass of the binary system and  $\hat{\mathbf{L}}$  the orbital angular momentum unit vector. It is convenient to define an *orbital* phase  $\phi = \int \omega_{orb} dt$  whose evolution is given by

$$v^3 \equiv \omega_{orb} M, \quad \frac{dv}{dt} = -\frac{F(v)}{dE/dv},\tag{3}$$

where  $F(v)$  and  $E(v)$  are respectively the flux emitted and the energy of a circular orbit with angular frequency  $\omega_{orb}$ , related to the main gravitational wave frequency  $f_{GW}$  via  $f_{GW} = \omega_{orb}/\pi$ .

By parametrizing the orbital angular momentum unit vector  $\hat{\mathbf{L}}$  as

$$\hat{\mathbf{L}} = (\sin \iota \cos \alpha, \sin \iota \sin \alpha, \cos \iota) \quad (4)$$

it is convenient to introduce the *carrier* phase  $\Psi$  given by

$$\frac{d\Psi}{dt} = \omega_{orb} - \cos \iota \frac{d\alpha}{dt}. \quad (5)$$

Numerically generated waveforms are usually decomposed in spherical harmonics, in particular the five quadrupolar modes ( $l = 2$ ) are the only non-vanishing at the lowest order in  $v$ , and the  $l = 2, m = \pm 2$  mode are the dominant ones. As determined by the PN analysis, the  $l = 2, m = 2$  mode in the inspiral phase  $h_{2,2}^{(insp)}$  (the only one which will be used here for comparison with test waveforms, which can be expressed in terms of the usual plus and cross polarizations as  $h_{2,2}^{(insp)} = h_+ - ih_\times$ ) is given by formulae which can be found e.g. in [31], which here we re-write in the following form

$$h_{2,2}^{(insp)}(t) = -2\sqrt{\frac{16\pi}{5}} \frac{\nu M}{d} v^2 \left[ \left( 1 - c(v) \frac{v^2}{42} (107 - 55\nu) \right) \left( \cos^4(\iota/2) e^{-2i(\Psi+\alpha)} + \sin^4(\iota/2) e^{2i(\Psi-\alpha)} \right) + \frac{\delta}{v^3} \sin \iota \left( \sin^2 \frac{\iota}{2} e^{i(\Psi-2\alpha)} + \cos^2 \frac{\iota}{2} e^{i(\Psi+2\alpha)} \right) \right] + O(v^5), \quad (6)$$

where spin-dependent terms in the amplitude have been neglected as well as terms of order higher than  $v^4$ ,  $t$ -dependence is understood in  $\Psi$  and  $\alpha$  and the  $z$ -axis used for defining  $l, m$  modes is parallel to the initial total angular momentum.

Note that differently from [31] and the previous version of the PhenSpin waveforms, the  $v^4$  terms have been added weighting them by a phenomenological function  $c(v)$  defined as

$$c(v) = \begin{cases} \exp \left[ -(1 - 0.05/\omega_{orb})^2 / 2 \right] & \omega_{orb} \leq 0.05 \\ 1 & \omega_{orb} > 0.05 \end{cases}$$

which has the role of turning  $v^4$  corrections on at values of the orbital frequency  $M\omega_{orb} \gtrsim 0.05$ , as otherwise poor matching with numerical simulations would be obtained.

The  $m = -2$  mode can be obtained via  $h_{2,-2}(\Psi) = h_{2,2}^*(\Psi + \pi)$  and in the equal mass case  $h_{2,-2} = h_{2,2}^*$  holds: we thus focus the calibration of our phenomenological model on the  $h_{2,2}$  mode.

The functions  $F(v)$  and  $E(v)$  are necessary to determine the orbital phase and they are known up to 3.5PN order as far as orbital effects are concerned, and up to 3PN and 2PN level for respectively  $\mathbf{S}_1 \mathbf{S}_2 \mathbf{L}$  and  $\mathbf{S}_1 \mathbf{S}_2, \mathbf{S}_1 \mathbf{S}_1, \mathbf{S}_2 \mathbf{S}_2$  interactions, see [32–34] for recent derivations of spin-orbit and spin-spin interaction effects.

According to studies in the non-spinning case [21, 35, 36], the TaylorT4 appears to be a very good approximant up to a frequency  $\bar{\omega} = \pi \bar{f}_{GW} \simeq 0.1/M$  for the equal mass case, even though its faithfulness seems to worsen for different mass-ratios (which however are not considered in this work). [45]

The PN evolution (6) is halted at  $t = t_m$ , when  $\omega_{orb}$  reaches the value  $\omega_m$  that is determined by comparison with the test waveforms. For  $\omega_{orb} > \omega_m$  ( $\omega_{orb}$  is monotonically increasing) the angular frequency is evolved according to

$$\omega_{orb}(t) = \frac{\omega_1}{1 - t/T_A} + \omega_0, \quad \omega_m < \omega_{orb} < z\omega_{rd} \text{ and } t_m < t < t_{rac}, \quad (7)$$

where the three unknown parameters  $\omega_{0,1}$  and  $T_A$  are determined by requiring continuity of  $\omega_{orb}$  and its first and second derivatives at the matching point defined by  $\omega_m$ .

The damped exponentials describing the ring-down phase are attached at the instant of time  $t_{rac}$  when  $\omega_{orb}$  reaches a fraction  $z$  of the  $\omega_{rd}$  value, the specific value of  $z$  has been determined like  $\omega_m$  by comparison with the numerical relativity waveforms, as described below, and differently with respect to the previous version of the PhenSpin waveforms, where  $z$  has not been fit to numerical simulations but kept constant to a convenient value.

Differently from the first PhenSpin version [25], where it has been kept constant at their value at  $t = t_m$ , the angular variable  $\alpha$  is evolved with a similar phenomenological formula

$$\frac{d\alpha}{dt} = \frac{\dot{\alpha}_1}{1 - t/T_A} + \dot{\alpha}_0, \quad (8)$$

where the parameters  $\hat{\alpha}_{1,0}$  are determined by requiring the continuity of  $\alpha$  up to its second derivative, and  $T_A$  is the same as determined in eq.(7).

Finally the usual ring-down description of the waveform is used

$$h_{2,2}^{(rd)}(t) = \sum_n e^{-t/\tau_n} A_n e^{i\omega_{rdn}t} \quad t > t_{rac}, \quad (9)$$

where it is used that the ring-down phase is described by adding damped exponentials of increasing inverse damping time, the overtones, with complex constants  $A_n$ 's. Here we assume that given the moderate spin values we are considering, the direction of the final spin of the black hole is parallel to the initial total angular momentum. We have checked that during the PN-inspiral phase ( $t < t_m$ ) this is indeed the case to very accurate precision (better than  $10^{-4}$ ) for all spin configurations considered here. In [42] the same numerical simulations used here are analyzed and a maximum misalignment angle  $\theta$  between the final spin and the initial total angular momentum is found to be around  $\theta \simeq 0.24\text{rad} \simeq 13^\circ$  (see fig.3 of [42]). Further investigations are necessary to assess the importance of this effect on the actual waveform shape.

Allowing more overtones requires to fix more coefficients, which can be done by admitting continuity of the waveform to the appropriate level: using  $n$  overtones requires matching the waveform up to its  $2 \times (n - 1)$ -th derivative, as each overtone involve the determination of a complex (or two real) constant parameter(s). The construction that inspired our work is the EOB matched to numerical relativity waveforms (usually referred to as EOBNR), introduced in [21] where the waveform is assumed circularly polarized (i.e.  $h_\times(\Psi + \pi/4) = \pm h_+(\Psi)$ ), so that the real and imaginary part of  $A_n$  for the  $l = 2, m = 2$  are not independent parameters. Here however we do not assume circular polarization, as in general terms of order  $v^3$  in eq.(6) (for unequal mass systems) will spoil this property and the stitching of the ring-down modes is performed independently on the real and imaginary part of each multipolar mode. For any such mode defined by a  $(l, m)$  pair there is an infinity of overtones with increasing damping factors, but for our practical purposes retaining only two overtones is enough.

As described in [43] each overtone with given  $l, m$  will be in general a superposition of the two modes which are usually designated by  $l, m$  and  $l, -m$ . Here we stick to the prescription adopted in [21] where only the  $m > 0$  mode is stitched to the inspiral waveform. We have verified that adding the  $l = 2, m = -2$  mode to  $h_{2,2}^{(rd)}$  would not improve the fit to the numerical waveforms, at the expense of introducing additional constant parameters which have to be fixed by imposing further continuity requirements.

The values of the ring-down frequencies and damping factors of the three lowest overtones of the  $l \leq 4$  modes can be read from [37] as a function of the mass and spin of the final object created by the merger of the binary system. We estimate the final mass by taking the algebraic sum of the constituents' masses and the negative binding energy once  $\omega_m$  is reached, and the final spin according to the phenomenological formula given in eq.(5) of [38].

The analytical waveforms just described have been quantitatively confronted with the set of test ones by computing the noise-less overlap integral

$$I_{\hat{h}_1, \hat{h}_2} \equiv 2 \int_0^\infty \left( \hat{h}_1(f) \hat{h}_2^*(f) + \hat{h}_1^*(f) \hat{h}_2(f) \right) df \quad (10)$$

maximized over initial phase and time of arrival, where normalized waveforms have been considered

$$\hat{h}(f) \equiv \frac{h(f)}{2} \left( \int_0^\infty |h(f)|^2 \right)^{-1/2}.$$

The angular frequency  $\omega_m$  and the parameter  $z$  have been determined by comparison with a first set of short test waveforms (4-6 cycles long) by picking the values maximizing the overlap integral (10) (with a precision respectively of  $\pm 5 \cdot 10^{-4}/M$  and 0.01). The set of short waveforms have initial orbital frequency  $\omega_{orb;ini} \sim 0.05/M$  (for comparison,  $\omega_{rd} \sim 0.3/M$ ). Note that despite  $\omega_{orb;ini}$  being not too far from the values of  $\omega_m$  obtained through the fit, see tab. I, it still allows at least one oscillation cycle before the onset of the phenomenological phase for all test waveforms.

The numerical waveforms in the set of test waveforms have been generated with **MayaKranc**. The grid structure for each run consisted of 10 levels of refinement provided by **CARPET** [39], a mesh refinement package for **CACTUS** [40]. Sixth-order spatial finite differencing was used with the BSSN equations implemented with **Kranc** [41]. The outer boundaries are located at  $317M$  and the finest resolution is  $M/77$ . Waveforms were extracted at  $75M$ . A few waveforms were generated at resolutions of  $\{M/64, M/77, M/90\}$ , and convergence consistent with our fourth order code is found. The short (long) runs showed a phase error on the order of  $5 \cdot 10^{-3}$  ( $5 \cdot 10^{-2}$ ) radians and an amplitude error of  $\approx 2\%$  ( $\approx 5\%$ ).

The numerical waveforms consist of two sets: the first set consisted in 24 few-cycle-long waveforms, representing mostly the merger and ring-down phases of a coalescence which, together with four phenomenological ones with

aligned spins, has been used as described above to fix the values of  $\omega_m$  and  $z$  for the corresponding values of initial spins. All of the numerical waveforms have initial spin  $\mathbf{S}_2/m^2 = (-0.6, 0, 0)$  in the reference frame in which the initial  $\hat{\mathbf{L}} = (0, 0, 1)$ . The different values of the first dimension-less spin have been obtained by rotating the  $(0, 0, 0.6)$  vector by 15 degrees in the x-z plane. This set of numerical waveforms has been completed by the addition of four phenomenological waveforms: one spin-less and three with spins aligned with the orbital angular momentum  $\mathbf{L}$  and the same magnitude as above (one with both spins aligned with  $\mathbf{L}$ , one with spins pointing in opposite directions and a third with both spins anti-aligned with  $\mathbf{L}$ ). Once determined the values of  $\omega_m$  and  $z$  for each waveform, their values for generic spins have been determined by assuming an analytical dependence on the dimension-less spin  $\chi_{1,2}$  defined as  $\chi_{1,2} \equiv \mathbf{S}_{1,2}/m_{1,2}^2$ , according to

$$\begin{aligned} M\omega_m = & a_0 + a_1(\chi_{1z} + \chi_{2z}) + a_2\delta(\chi_{1z} - \chi_{2z}) + a_3(\chi_1\chi_2) + \\ & a_4(\chi_1^2 + \chi_2^2) + a_5(\chi_{1z}\chi_{2z}) + a_6(\chi_{1z}^2 + \chi_{2z}^2) + (\chi_{1z} + \chi_{2z}) \times \\ & [a_7(\chi_1\chi_2) + a_8(\chi_1^2 + \chi_2^2) + a_9(\chi_{1z}\chi_{2z}) + a_{10}(\chi_{1z}^2 + \chi_{2z}^2)] \dots, \end{aligned} \quad (11)$$

where the spin components are understood in a frame where the orbital angular momentum is along the  $z$  axis and higher powers of the spin components have been neglected. From eq. (11) one can note that since spins are evolving in time,  $\omega_m$  is also slightly changing with time, the explicit values taken by the  $a_i$  coefficients are reported in tab. II. The  $\chi_i$  values used to fit  $\omega_m$  are taken at  $t = t_m$ .

The dependence of the  $\omega_{orb}$  evolution equation on  $\mathbf{L}$  and  $\mathbf{S}_{1,2}$  implies that the spin components parallel to the orbital angular momentum enter already at linear level, whereas the dependence on the spin components in the plane of the orbit starts from the quadratic level. The  $a_i$  coefficients may depend on the symmetric mass ratio  $\nu$ , but it is assumed here that they can be analytically expanded around their value at  $\delta = 0$ , according to

$$a_i(\delta) = a_i + \delta a_i^{(1)} + \delta^2 a_i^{(2)} + \dots \quad (12)$$

Note that anti-symmetric combinations of spin components do not appear for  $\delta = 0$ . Given the specifics of the test waveform set we used (all having  $\delta = 0$ ) we could not calculate the coefficients  $a_i^{(i)}$  nor  $a_2$ . An analog formula has been assumed for  $z$

$$\begin{aligned} z = & b_0 + b_1(\chi_{1z} + \chi_{2z}) + b_2\delta(\chi_{1z} - \chi_{2z}) + b_3(\chi_1\chi_2) + \\ & b_4(\chi_1^2 + \chi_2^2) + b_5(\chi_{1z}\chi_{2z}) + b_6(\chi_{1z}^2 + \chi_{2z}^2), \end{aligned} \quad (13)$$

where terms cubic in the spins have not been necessary here. Results from the fit of  $z$  are reported in tab. II.

These values have then been tested by computing the *faithfulness* of the now fully calibrated PhenSpin waveforms with respect to a second set of long waveforms, consisting of 8 long numerical waveforms (12-15 cycles long) plus the 10 phenomenological ones: 4 with the same parameters as above (initial  $\omega_{orb} \simeq 0.03/M$ ) and six additional ones characterized by spins aligned with the angular momentum and chi-pair values give by  $(\chi_{1z}, \chi_{2z}) = \{(0.3, 0.3), (0.3, -0.3), (-0.3, -0.3), (0.8, 0.8), (0.8, -0.8), (-0.8, -0.8)\}$ . The faithfulness of a pair of waveforms  $(h_1, h_2)$  is quantified by the noise-weighted version of the overlap integral 10, which we rewrite in terms of  $\epsilon$ , the *mismatch* parameter (see e.g. [44])

$$1 - \epsilon \equiv \frac{\int_0^\infty \frac{h_1(f)h_2^*(f) + h_1^*(f)h_2(f)}{S_n(f)} df}{2 \left( \int \frac{|h_1(f)|^2}{S_n(f)} df \right)^{1/2} \left( \int \frac{|h_2(f)|^2}{S_n(f)} df \right)^{1/2}}, \quad (14)$$

where maximization over initial phase and arrival time is understood and  $S_n(f)$  is the single-sided power spectral density of Advanced LIGO strain noise and waveforms are normalized with respect to noise weighted integrals. The results of the above integrals comparing PhenSpin waveforms and long test waveforms with identical physical parameters are described in the next section.

### III. RESULTS

The analytical waveforms have been calibrated by comparison with 28 short test waveforms described in the previous section and the results obtained by maximizing the overlap given by eq. (10) are reported in tab. I. The

determination of the  $\omega_m$ 's giving the best overlap for different spin values allowed to evaluate some of the coefficients in the phenomenological formulae (11) and (13), as given in tab. II.

Once fixed the value of  $\omega_m$  and  $z$  for generic spin values, it is possible to generate analytical waveforms with any specific initial condition without any further tuning: the value of  $\omega_m, z$  will be determined analytically via eqs. (11) and (13) with the unknown coefficients arbitrarily set to zero. It is then possible to generate waveforms with no tunable parameters for comparison with the second set of long waveforms. The results of the faithfulness integrals described in eq. (14) are reported in fig. 1 for the range of masses 60-100  $M_\odot$ . The lower range corresponds to the minimal mass value enabling the long waveforms to start at a physical frequency which is smaller than the lower edge of the sensitive band (which we assume to be around 20Hz) whereas beyond the upper range value only the ring-down phase is in-band (for reasonable distances of the sources).

#### IV. CONCLUSIONS

We presented an analytical method to produce complete gravitational waveforms from spinning coalescing binaries. The free parameters of the model are the values of the orbital frequency at the transition from the inspiral to the phenomenological phase and at the transition from the phenomenological to the ring-down phase. After a calibration process involving the dominant multipolar mode obtained by numerical relativity and other phenomenological construction from a different family, all the parameters have been fixed and the PhenSpin are ready to use, once fed with the physical parameters of the coalescing binaries (mass, spins, inclination angles, initial phase). We computed noise-weighted overlap integral obtaining values between 0.95 and 0.98 for a wide range of masses. Further investigations are necessary in order to assess how such mismatch can affect the precision of parameter estimation performed via these family of waveforms.

#### Acknowledgments

It is a pleasure to thank the organizers of the NRDA conference in Waterloo for the stimulating scientific environment created by the meeting. This work was supported by the FAI grant from INFN and by the NSF grant PHY-0653550, PHY0955773, PHY-0925345, PHY-0941417 and PHY-0903973, PHY0955825, TG-PHY060013N.

#### References

- 
- [1] B. Abbott *et al.* [ LIGO Scientific Collaboration ], Rept. Prog. Phys. **72** (2009) 076901. [arXiv:0711.3041 [gr-qc]].
  - [2] F. Acernese, M. Alshourbagy, P. Amico, F. Antonucci, S. Aoudia, K. G. Arun, P. Astone, S. Avino *et al.*, Class. Quant. Grav. **25** (2008) 184001.
  - [3] B. Willke [ LIGO Scientific Collaboration ], Class. Quant. Grav. **24** (2007) S389-S397.
  - [4] L. Blanchet, Living Rev. Rel. **9** (2006) 4.
  - [5] S. A. Teukolsky, Astrophys. J. **185** (1973) 635.
  - [6] F. Pretorius, Phys. Rev. Lett. **95** (2005) 121101 [arXiv: gr-qc/0507014].
  - [7] M. Campanelli, C.O. Lousto, P. Marronetti, and Y. Zlochower, Phys. Rev. Lett. **96** (2006) 111101 [arXiv:gr-qc/0511048].
  - [8] J.G. Baker, J. Centrella, D. Choi, M. Koppitz and J. van Meter, Phys. Rev. Lett. **96** (2006) 111102 [arXiv:gr-qc/0511103].
  - [9] F. Herrmann, I. Hinder, D.M. Shoemaker, P. Laguna and R.A. Matzner, Phys. Rev. D **76** (2007) 084032 [[arXiv:0706.2541]].
  - [10] W. Tichy and P. Marronetti, Phys. Rev. D **78** (2008) 081501 [arXiv:0807.2985 [gr-qc]].
  - [11] M.A. Scheel, M. Boyle, T. Chu, L.E. Kidder, K.D. Matthews, H.P. Pfeiffer Phys. Rev. D **79** (2009) 024003 [arXiv:0810.1767 [gr-qc]].
  - [12] J. G. Baker, W. D. Boggs, J. Centrella, B. J. Kelly, S.T. McWilliams and J.R. van Meter, Phys. Rev. D **78** (2008) 044046 [arXiv:0805.1428 [gr-qc]].

#	Overlap	$M\omega_m \times 10^2$	$z$	$M\omega_{rd} \times 10^2$
1	0.992	5.50	0.76	29.6
2	0.990	5.50	0.80	29.2
3	0.989	5.50	0.85	28.8
4	0.979	5.40	0.85	28.4
5	0.976	5.75	0.85	27.9
6	0.978	5.90	0.78	27.4
7	0.986	5.95	0.85	26.9
8	0.991	6.20	0.85	26.4
9	0.992	6.15	0.84	26.0
10	0.991	6.25	0.80	25.7
11	0.993	6.20	0.85	25.6
12	0.993	6.20	0.83	25.7
13	0.993	6.15	0.81	26.0
14	0.990	6.25	0.80	26.5
15	0.983	6.20	0.80	27.2
16	0.989	5.95	0.85	27.9
17	0.985	6.15	0.80	28.6
18	0.988	5.82	0.83	29.1
19	0.984	6.00	0.78	29.6
20	0.985	5.75	0.80	29.9
21	0.984	5.50	0.83	30.1
22	0.991	5.50	0.80	30.1
23	0.992	5.45	0.77	30.1
24	0.992	5.47	0.81	29.9
25	0.992	5.55	0.84	26.9
26	0.992	6.05	0.74	29.0
27	0.993	5.20	0.85	26.9
28	0.988	5.30	0.80	23.6

Table I: Values of the overlap integral given by eq.(10) between the analytical and the 28 test waveforms: the first 24 are numerically generated, with initial conditions  $\mathbf{S}_1/m_1^2 = (\sin \alpha, 0, \cos \alpha)$  and  $\mathbf{S}_2/m_2^2 = (-0.6, 0, 0)$ , with  $\alpha = (k - 1) \times \pi/12$  for  $0 < k \leq 24$ , the following 4 have spins parallel to the orbital angular momentum with components respectively  $(S_{1z}, S_{2z})/m^2 = (0, 0), (0.6, 0.6), (0.6, -0.6), (-0.6, -0.6)$ . In the columns from third to fifth the values of  $\omega_m$  and  $z$  maximizing the overlap and of  $\omega_{rd}$  are reported.

$\omega_m$ -Coeff.	$\omega_m$ fit ( $\times 10^{-3}$ )	$z$ -Coeff.	$z$ fit ( $\times 10^{-2}$ )
$a_0$	55.500	$b_0$	84.00
$a_1$	0.997	$b_1$	-2.15
$a_3$	-2.032	$b_3$	-4.42
$a_4$	5.629	$b_4$	-2.64
$a_5$	8.646	$b_5$	-5.88
$a_6$	-5.909	$b_6$	-2.21
$a_7$	1.801		
$a_7$	-14.059		
$a_8$	15.483		
$a_9$	8.922		

Table II: Coefficients of eqs. (11) and (13) as determined by comparison of the analytical waveforms with the 28 short test waveforms.

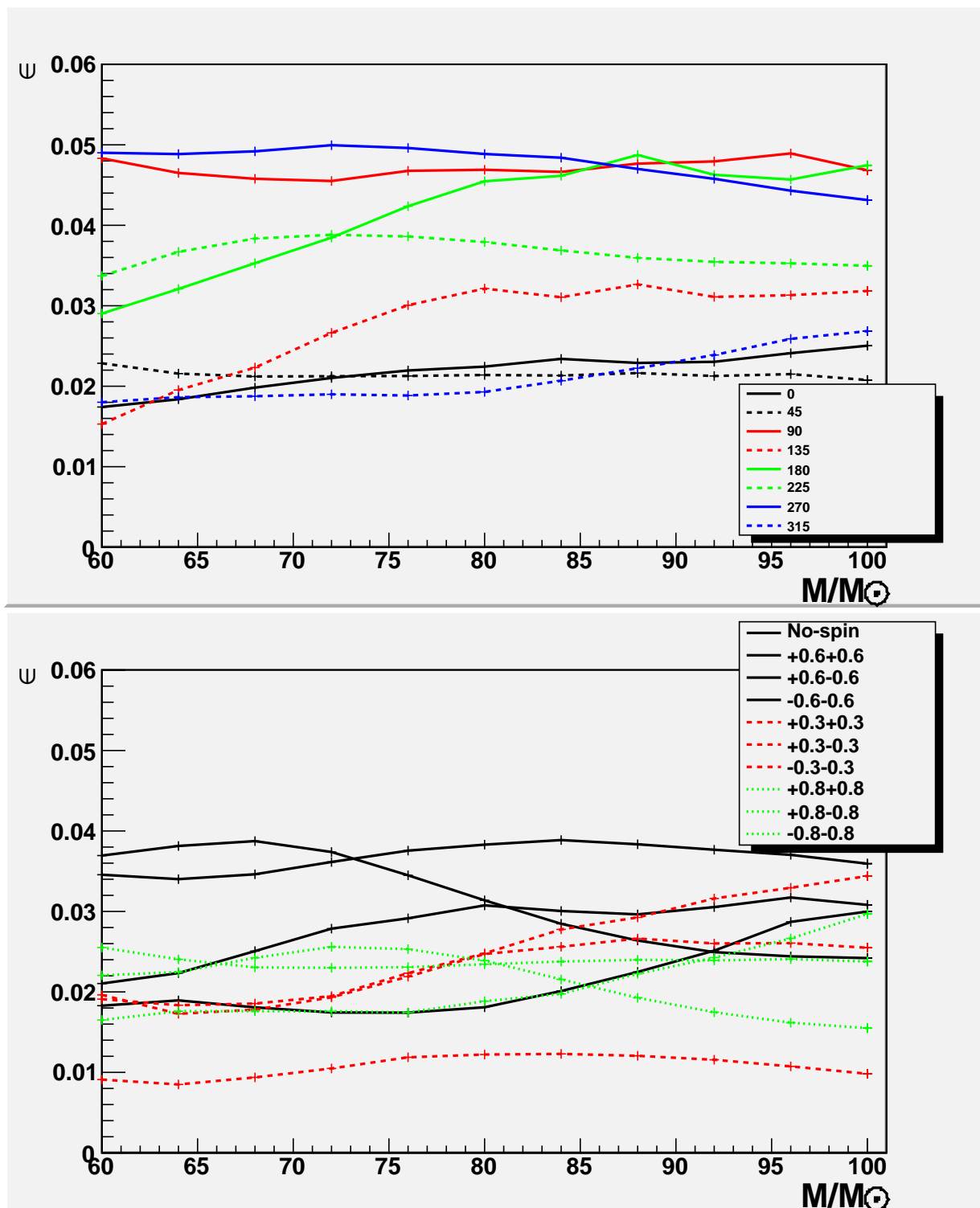


Figure 1: Quantitative comparison between the calibrated PhenSpin waveforms and the numerical relativity ones (top) and phenomenological waveforms (bottom). The labels in the upper figure denote the angle (degrees) between the initial  $\mathbf{S}_1$  and the z-axis, the labels in the lower one denote the spin value along the z-axis of  $\mathbf{S}_1$  and  $\mathbf{S}_2$  in units of  $m_i^2$ .



- [13] P. Ajith *et al.*, *Class. Quant. Grav.* **24** (2007) S689 [arXiv:0704.3764 [gr-qc]]; P. Ajith *et al.*, *Phys. Rev. Lett.* **106**, 241101 (2011); arXiv:0909.2867 [gr-qc].
- [14] C.O. Lousto, H. Nakano, Y. Zlochower and M. Campanelli, *Phys. Rev. D* **81** (2010) 084023 [arXiv:0910.3197 [gr-qc]].
- [15] D. Pollney *et al.*, *Phys. Rev. D* **76** (2007) 124002 [arXiv:0707.2559 [gr-qc]].
- [16] M. Hannam, *Class. Quant. Grav.* **26** (2009) 114001 [arXiv:0901.2931 [gr-qc]].
- [17] S. Husa, *Eur. Phys. J. ST* **152** (2007) 183–207.
- [18] F. Pretorius, “Physics of Relativistic Objects in Compact Binaries: From Birth to Coalescence”, Springer, Heidelberg (Germany), 2009 [arXiv:0710.1338].
- [19] J. Abadie *et al.* [The LIGO Scientific Collaboration and the Virgo Collaboration and the Virgo], *Phys. Rev. D* **83** (2011) 122005 [arXiv:1102.3781 [gr-qc]].
- [20] A. Buonanno and T. Damour, *Phys. Rev. D* **59** (1999) 084006 [arXiv:gr-qc/9811091]; A. Buonanno, T. Damour, *Phys. Rev. D* **62**, 064015 (2000) [arXiv: gr-qc/0001013]; T. Damour, P. Jaranowski, G. Schaefer, *Phys. Rev. D* **62**, 084011 (2000) [arXiv: gr-qc/0005034].
- [21] A. Buonanno, G. B. Cook and F. Pretorius, *Phys. Rev. D* **75** (2007) 124018 [arXiv:gr-qc/0610122].
- [22] A. Buonanno, Y. Pan, J. G. Baker, J. Centrella, B. J. Kelly, S. T. McWilliams and J. R. van Meter, *Phys. Rev. D* **76** (2007) 104049 [arXiv:0706.3732 [gr-qc]].
- [23] T. Damour and A. Nagar, *Phys. Rev. D* **79** (2009) 081503 [arXiv:0902.0136 [gr-qc]].
- [24] Y. Pan, A. Buonanno, L. T. Buchman, T. Chu, L. E. Kidder, H. P. Pfeiffer and M. A. Scheel, arXiv:0912.3466 [gr-qc].
- [25] R. Sturani, S. Fischetti, L. Cadonati *et al.*, *J. Phys. Conf. Ser.* **243**, 012007 (2010). [arXiv:1005.0551 [gr-qc]].
- [26] Y. Pan, A. Buonanno, Y. -b. Chen *et al.*, *Phys. Rev. D* **69** (2004) 104017; [gr-qc/0310034].
- [27] A. Buonanno, Y. -b. Chen, Y. Pan, M. Vallisneri, *Phys. Rev. D* **70** (2004) 104003; [gr-qc/0405090].
- [28] D. A. Brown, J. Crowder, C. Cutler *et al.*, *Class. Quant. Grav.* **24** (2007) S595-S606. [arXiv:0704.2447 [gr-qc]].
- [29] <https://www.lsc-group.phys.uwm.edu/daswg/projects/lal.html>
- [30] A. Buonanno, B. Iyer, E. Ochsner, Y. Pan and B. S. Sathyaprakash, *Phys. Rev. D* **80** (2009) 084043 [arXiv:0907.0700 [gr-qc]].
- [31] K. G. Arun, A. Buonanno, G. Faye and E. Ochsner, *Phys. Rev. D* **79** (2009) 104023 [arXiv:0810.5336 [gr-qc]].
- [32] B. Mikoczi, M. Vasuth, L. A. Gergely, *Phys. Rev. D* **71** (2005) 124043. [astro-ph/0504538].
- [33] E. Racine, A. Buonanno and L. E. Kidder, *Phys. Rev. D* **80** (2009) 044010 [arXiv:0812.4413 [gr-qc]].
- [34] L. Blanchet, A. Buonanno and G. Faye, arXiv:1104.5659 [gr-qc].
- [35] J. G. Baker, J. R. van Meter, S. T. McWilliams, J. Centrella and B. J. Kelly, *Phys. Rev. Lett.* **99** (2007) 181101 [arXiv:gr-qc/0612024].
- [36] M. Boyle *et al.*, *Phys. Rev. D* **76** (2007) 124038 [arXiv:0710.0158 [gr-qc]].
- [37] E. Berti, V. Cardoso and C. M. Will, *Phys. Rev. D* **73** (2006) 064030 [arXiv:gr-qc/0512160].
- [38] E. Barausse and L. Rezzolla, *Astrophys. J.* **704** (2009) L40 [arXiv:0904.2577 [gr-qc]].
- [39] E. Schnetter, S.H. Hawley and I. Hawke, *Class. Quant. Grav* (2004) **21** 1465–1488 [arXiv:0310042 [gr-qc]].
- [40] Cactus Computational Toolkit home page: <http://www.cactuscode.org>.
- [41] S. Husa, I. Hinder and C. Lechner, *Computer Physics Communications* **174** (2006) 983-1004 [arXiv:0404023 [gr-qc]].
- [42] S. Fischetti, J. Healy, L. Cadonati, L. London, S. R. P. Mohapatra, D. Shoemaker, *Phys. Rev. D* **83** (2011) 044019. [arXiv:1010.5200 [gr-qc]].
- [43] E. W. Leaver, *Proc. Roy. Soc. Lond.* **A402** (1985) 285-298; E. Berti, V. Cardoso, C. M. Will, *Phys. Rev. D* **73** (2006) 064030. [gr-qc/0512160].
- [44] B. J. Owen, *Phys. Rev. D* **53**, 6749-6761 (1996). [gr-qc/9511032].
- [45] For comparison  $f_{GW} \simeq 65 Hz \left(\frac{\omega M}{0.01}\right) \left(\frac{M}{10M_{\odot}}\right)^{-1}$ .